MODIFIED DOLOMITE-BASED PELLETS FOR HIGH TEMPERATURE POST-COMBUSTION CO_2 CAPTURE

Ainara Moral[1*], Anne Charlotte Wold[1], Kumar Ranjan Rout[1,2], De Chen[1]

[1] Department of Chemical Engineering, Norwegian University of Science and Technology (NTNU), Sem Sælands vei 4, N-7491 Trondheim, Norway

[2] SINTEF Industry, Norway

* Corresponding author e-mail: ainara.moral.larrasoana@ntnu.no

Abstract

In this study, synthetic dolomite-based pellets were prepared by means of one-pot method. Zr and Ce were used as modifier and aluminate cement was employed as binder. The addition of the promoters by two different routes (1-step or 2-step) was analyzed. The pellets were exposed to several carbonation-calcination cycles in a thermogravimetric analyzer at low CO_2 concentration (5 vol.%) and wet conditions (8 vol.% steam) at 600 ºC. The calcination was carried in harsh conditions to mimic the realistic process (950 ºC, 77 vol.% CO_2). The Zr-modified and synthetized by 2-step one-pot method was presented as the most promising among all the sorbents with an initial capturing capacity of 16.9 % in cycle 2 to 14.4 % after cycle 40. It was proved that both, sintering and pore blockage are fairly well prevented. Different characterization techniques were employed, including N_2 adsorption-desorption at 77 K, X-ray diffraction (XRD) and scanning electron microscopy combined with energy-dispersive spectroscopy (SEM-EDS).

Keywords: *Calcium-Looping; dolomite; cement; zirconium*

1. Introduction

Carbon capture and storage (CCS) was identified by the International Energy Agency (IEA) as a crucial technology to reach the mitigations requirements targeted by United Nations in the Paris agreement in 2015 [1], where the target of keeping temperature increase below 2 °C (above pre-industrial levels) was agreed. As a result, approximately 48 % of the CO_2 emission reduction will come from power plants [2]. Within the CCS technologies, post-combustion CO_2 capture has raised among the best processes to be implemented in the existing power plants. Currently, the most mature technology employed industrially is the Monoethanolamin Absorption (MEA). However, several problems associated such as, low total efficiency as a result of the extraction of steam in the solvent regeneration [3], solvent degradation [4] or corrosion [5] and the high cost [6] makes necessary to find new technologies.

A promising alternative is the calcium-looping (CaL), consisting of a first carbonation step with calcium oxide-based sorbent, following by the regeneration of the sorbent at high temperature in a calciner. The interest on this process has increased due to its potential to achieve a lower energy penalty than the one reached in the MEA. The application of this technology have been investigated in cement [7], coal-fire [8] and Natural Gas Combined Cycle (NGCC) power plants [9] .

Several studies have been done to evaluate the performance of the CO_2 capture by CaL on the NGCC power plants [9–14]. A significant challenge associated with the combination of the processes are the higher energy requirement due to lower CO_2 concentration in the flue gas (4 vol.%) and consequently, lower temperature (600 ºC) in the carbonator comparing to the coal fire plants (650 ºC and 15 vol.%). On the other hand, steam will be a subproduct in combustion flu gas (5-10 vol.%) [15], which will influence the capturing efficiency. Furthermore, the process requirement of harsh calcination conditions (>80 vol.% CO_2, T>900 °C) must be taken into account in the sorbent evaluation [16].

Environmental and economic factors regarding the nature of sorbents hinders the development of the CaL. Therefore, the necessity of cost efficient environmentally friendly sorbent is significant for the overall cost. The use of calcium sorbents based on natural resources [17], mainly limestone ($CaCO_3$) and dolomite ($CaCO_3.MgCO_3$) might solve this problems. However, they suffer a rapid decrease in CO_2 sorption capacity with an increasing number of carbonation/calcination cycles mainly due to sintering and pore collapse. Dolomite presents a significantly lower capacity than limestone, however, its lower decomposition temperature and higher resistance to sintering, due to the action of MgO as a thermally stable support mitigating the capacity loss [18], makes it a promising raw material.

Large efforts have been carried out for enhancing the natural sorbents uptake capacity and stability [19]. An interesting approach in material development is the incorporation of inert supporting materials with high melting points. In this respect, Zr modified sorbents have been extensively investigated showing a notable stability over several cycles, attributed to the formation of the thermally resistant $CaZrO_3$ when CaO reacts with ZrO_2

[20–24]. On the other hand, the possibility of using CeO_2 as modifier have been less investigated although its stabilizer effect by creating a physical barrier has been trusted. It has been suggested that the release of O^{2-} from the surface of CeO_2 can facilitate the reaction of CaO with CO_2 [25]. Aluminate cement has been previously reported as a good and inexpensive support for pelletization [26–30], owing to the formation of calcium-aluminum oxides (specially mayenite) from the solid reaction of Al_2O_3 and CaO that results in the formation of a solid and inert framework which prevents the sintering and acts as mechanical stabilizer.

Beside the composition, the preparation method have a big impact on the sorbent properties. In the literature several methods have been proposed. Unfortunatley, most of them having disadvantages associated with expensive and challenging preparation methods and consequently, making difficult the scale up of the synthesis [31].

In this work, a one pot method has been proposed in order to produce active and stable dolomite based modified pellets for CaL. The addition of two dopants has been investigated, including Zr and Ce. Finally, the optimization of the synthesis has been investigated by the analyzes of two simple routes using the one pot method.

2. Experimental procedure

2.1. Materials

Dolomite (AGRI Hagekalk supplied by Franzefoss Miljøkalk) was employed as CaO source, aluminate cement (Cement FONDU, Al_2O_3>37%, CaO <39.8%, SiO_2<6 %, <18.5%) as binder and two different additives were used as modifiers including zirconyl nitrate solution (35 wt. % in dilute nitric acid) and Cerium(III) nitrate hexahydrate as Zr and Ce precursors respectively.

2.2. Sorbent preparation

Dolomite based pellets were prepared by means of one pot method. Two different routes, depending on how the addition of the raw materials was done, were studied. In the first route, calcined and milled dolomite (800 ºC for 6 h, dp<90 µm) was impregnated by means of incipient wetness impregnation with the precursor solution (Zr or Ce). Subsequently, the dry impregnated solid and the dry cement were milled together until a homogeneous solid mixed was obtained. Finally, water was sprayed slowly with a continuous stirring until the pellets were formed (2S method). Conversely, in the second route, the calcined and milled dolomite and dry cement were previously mixed until a homogeneous solution was gotten. The solid mixture was impregnated by wetness impregnation and finally, water was sprayed until the pellet were formed (1S method). The obtained pellets were aged for 4-7 days until a hard solid was formed. Finally, the calcination of the pellets was done at 950 ºC for 6 hours.

2.3. Cycling stability

The capture capacity of the sorbents along carbonation-calcination cycles was measured in a common thermogravimetric analyzer (Linseis Thermal Analysis STA PT1600). A small quantity (10-15 mg) of sorbent was placed in a sample holder. The sample was initially heated up until 900 °C in air/Ar atmosphere (200 cm^3/min) in order to remove possible humidity and CO_2 adsorbed. The carbonation reaction was carried out at CO_2 partial pressure of 5 vol.% CO_2 and 8 vol.% H_2O (air/Ar balance) at a temperature of 600 °C for 30 minutes. Subsequently, the temperature was increased until 800 ºC in 5 vol.% CO_2 (air/Ar balance). Finally, the atmosphere was changed to 77 vol.% CO_2 and the temperature was increased until 950 °C, where it was kept for 5 minutes, simulating the real calcination conditions.

The capture capacity was calculated assuming the weight change showed in TGA analyzed was due to the carbonation or calcination of the sorbent.

2.4. Characterization

Fresh and spent sorbents were characterized by different techniques including, N_2 adsorption-desorption at 77 K, X-ray diffraction (XRD) and emission scanning electron microscopy combined with energy-dispersive spectroscopy (SEM-EDS).

N_2 adsorption-desorption isotherms were measured in a Micrometrics TriStar 3020 automatic volumetric analyzer at 77 K, with previous preconditioning of the samples at 300 °C for 2 h and vacuum. The surface area of the different samples was determined using the Brunauer-Emmett-Teller (BET) method, and the pore size distribution was calculated using the Barrett-Joyner-Halenda (BJH) method.

XRD experiments were performed at ambient temperature on a D8-Focus diffractometer equipped with the Cu Kα radiation (λ = 0.15418 nm) X-ray source. XRD patterns were examined with 2θ values ranging from 5° to 75° with a step of 0.02 ° and a signal accumulation period of 1 s per step.

Lastly, the morphological analysis was completed using field emission scanning electron microscopy (SEM), (FEI APREO) coupled with an EDS detector (Oxford).

3. Results and discussion

3.1. Sorbents

Table 1 summarizes the synthetized materials, including, sample, employed route (1- or 2-step) as well as the content (% wt) of the different modifiers, including Zr, Ce and Al (from cement, assuming that aluminate cement consists of CaO and Al_2O_3). Additionally, calcined and milled dolomite (800 ºC for 6 h, d_p< 90 µm) was used as reference to compare the performance of the synthetic sorbents tested in a size range of 500-850 µm.

Table 1: Summary of the different prepared sorbent

Sample	Meth.	Zr (wt. %)	Ce (wt. %)	Al (wt. %)
1S(5.5Zr,10Al)	1-step	5.5	-	10
2S(5.5Zr,10Al)	2-step	5.5	-	10
2S(5.5Ce,10Al)	2-step	-	5.5	10
1S(15Al)	1-step	-	-	15

3.2. Cycling stability

Capturing capacity (%) over cycles under experimental conditions described in 2.3 is represented in Figure 1. As expected, calcined dolomite presented a pronounced fast loss in capacity from 38.4 % of initial capturing capacity to 19 % after only 15 cycles and to 13 % after 40 cycles and which expected to decrease until a very low residual values around 10 % [18]. Conversely, a strong improvement on the stability was observed in the synthetic sorbents. The 2S sorbents prepared with both modifiers, Ce and Zr, presented a similar initial capacity (~19 %). Nevertheless, its performance throughout cycles varied significantly. The sorbent containing Cerium exhibited a minor initial increase in the capturing capacity from cycle 1 to cycle 2. However, it gradually decreased from 21.6 % in cycle 2 to 16.5 % of capture capacity in cycle 15. By contrast, the homologous sorbent modified with Zr 2S(5.5Zr,10Al) presented a slightly initial decrease in capacity to later show relatively stable behavior (from 16.9 % in cycle 2 to 15.5 % in cycle 15 and 14.4 % in cycle 40). On the other hand, comparing both Zr-modified sorbents with same composition but prepared by the different routes (1S and 2S) a noticeable difference, especially in terms of activity, was observed. Around 2 % lower capacity was found for 1S(5.5Zr,10Al) than for 2S(5.5Zr,10Al) and a slightly higher capacity lost (22.0 % and 15.1 % from 2-40 respectively) over 40 carbonation-regeneration cycles tested. This is surprising considering that the CaO from cement is inactive in the carbonation [26], hence, it was expected to observe more active CaO sites and therefore, higher capture capacity, in the 1S(5.5Zr,10Al) sorbent compared to the sorbent made by 2S route, where all the Zr was directly impregnated in the active CaO sites to form $CaZrO_3$.

Finally, the sorbent supported on cement (1S(15Al)) presented an initial capacity of 14.5 % and a loss in capacity of 17.4 % through 15 cycles (2-15). This would prove that the addition can be also beneficial for the stability of the sorbent. However, the combination of Zr and cement appears as the most beneficial combination in order to obtain a sorbent with relatively good activity and stability. Furthermore, the synthesis realized by 2-step has been found as the best route.

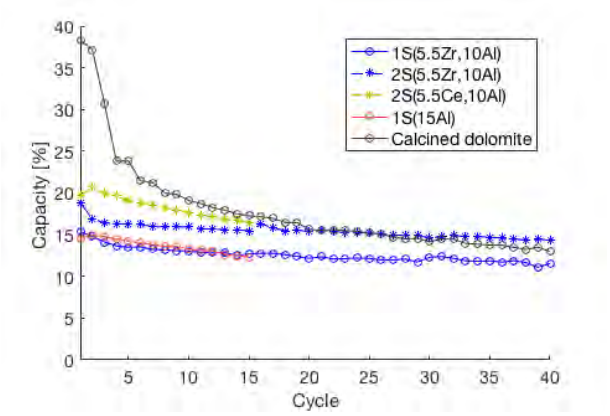

Figure 1. Capturing capacity (%) as a function of carbonation-calcination cycles for calcined dolomite, 1S(5.5Zr,10Al), 2S(5.5Zr,10Al), 2S(5.5Ce,10Al) and 1S(15Al) (Carb: F_T=400 mL/min, 5 % CO_2, 8 % H_2O, T_{carb}= 600 °C, t=30 min; Calc: 77 % CO_2 (N_2/Ar), T_{calc}= 950 °C, t=5 min)

3.3. Characterization

The chemical composition was assessed by XRD. The patterns of the synthetic pellets, calcined dolomite and dry cement are depicted in Figure 1.

The crystallographic phases corresponding to CaO and MgO were mainly detected in calcined dolomite, however, small signals corresponding to $Ca(OH)_2$ and $CaCO_3$ were also distinguished, possibly due to water and CO_2 adsorbed during the cooling down post-calcination. The diffractogram of dry cement revealed the presence of different calcium aluminates phases, including mainly $CaAl_2O_4$, and $Ca_3Al_2O_6$. Furthermore, two more phases were identified in the cement diffractogram, Fe_2O_3 and SiO_2, as it was indicated in the specifications of FONDU cement. As expected, the formation of mayenite was observed in all prepared sorbents, as it has been reported by several authors when aluminate cement is used as binder [26–30], indicating the solid state reaction between CaO and Al_2O_3 oxides forming the inert framework.

For the sorbents modified with Zr, the presence of $CaZrO_3$ was confirmed verifying the reaction of ZrO_2 with CaO [32], which improves the durability of the sorbents by means of the action of $CaZrO_3$ as a barrier against sintering. Oppositely, when Ce was used as modifier, CeO_2 was recognized, indicating the absence of reaction of CaO with the modifier [25] . Furthermore, comparing the Ce and Zr modified sorbents, the lasts one presented a more intense mayenite ($Ca_{12}Al_{14}O_{33}$) peaks, which can indicate a stronger formation of the inert solid framework preventing better the sintering, than in the Ce-modified sorbent, where a more pronounced deactivation was observed. There were not major differences between the patterns of fresh and spent samples, nor comparing the sorbents prepared by 2 different methods (1- or 2- step).

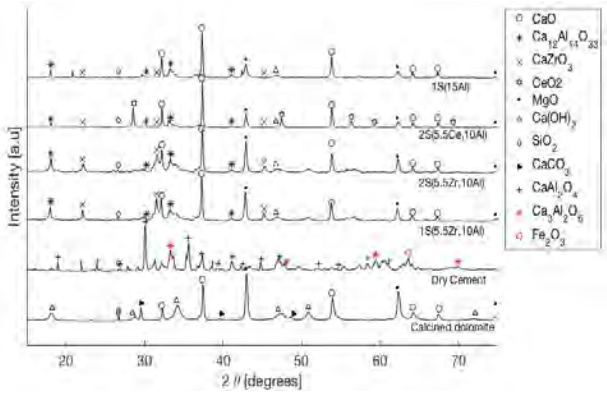

Figure 2: XRD patterns of calcined dolomite, cement, and modified sorbents (1S(5.5Zr,10Al), 2S(5.5Zr,10Al), 2S(5.5Ce,10Al) and 1S(15Al))

On the other, Table 2 shows the CaO crystal sizes calculated by Scherrer equation [33] and BET surface of all the sorbents. Calcined dolomite presented the smallest CaO crystal size (40.4 nm) comparing to the modified sorbents (46.5-54 nm). However, it suffered a pronounced increase of CaO crystal size in only 15 cycles (47.6 nm), demonstrating that sintering is the main deactivation mechanism, as was also previously reported [18]. Among the synthetized sorbents, 2S(5.5Ce,10Al) presented the highest CaO crystal size (54.0 nm), possibly due to a slightly higher sintering during the pre-calcinations step. However, it appears that this difference does not have considerable impact in the initial capturing capacity as was previously seen (Figure 1). Hence, the CaO crystal sizes in this range, does not result in any significative effect in the capture capacity. Furthermore, the spent samples were analyzed (not shown), not showing a noticeable difference regarding CaO crystal sizes observed, nor to the crystal phases found, indicating that sintering was well prevented in the modified sorbents.

Table 2**:** CaO crystal sizes (nm) and BET surface area (m^2/g) for calcined dolomite and and modified sorbents (1S(5.5Zr,10Al), 2S(5.5Zr,10Al), 2S(5.5Ce,10Al) and 1S(15Al))

Sample	CaO Crystal Size (nm)	S_{BET} (m^2/g)
Calcined Dolomite	40.4	21.0
1Sa(5.5Zr,10Al)	46.5	8.8
2Sa(5.5Zr,10Al)	49.0	10.6
2S(5.5Ce,10Al)	54.0	7.2
1S(15Al)	49.6	11.4

It is known that sorbents porosity plays an important role in the gas–solid reaction, since the diffusion inside particles has a strong dependency on the pore structure [34]. The BET surface areas of dolomite and modified sorbents are summarized in Table 2. It was clearly seen that calcined dolomite presented higher surface area ($21.0\ m^2/g$) comparing to synthetic sorbents ($7.2\text{-}11.4\ m^2/g$). This can be attributed to the lower sintering suffered during lower degree of pre-calcination as well as related to the addition of dopants and cement [35,36]. Regarding to Zr and Ce-doped sorbents, a clear relation between the capturing capacity and surface area was observed, being 2S(5.5Zr,10Al) the sorbent with higher surface area ($10.6\ m^2/g$), the one which presented higher activity in the CO_2 capture. However, this trend was not followed by the sorbent 1S(15Al), which with the highest surface does not appear as the most active.

Nevertheless, not only the surface areas have an important effect in the sorbent performance, but also changes in the pore distribution can significantly affect to the stability. Indeed, Chen et al. [37] reported that the pore size distribution has a more critical role than the surface area and the pore volume. Hence, the pore size distribution of calcined dolomite and Zr modified sorbents are represented in Figure 3. Both calcined dolomite and the Zr-doped sorbents presented a bimodal distribution, with peaks in the small range of mesopores (3-4 nm) as well as in the big mesopores and macropores range (20-150 nm). A similar tendency was also reported by other authors [30,38].

More mesopores with small size (3-4 nm) were identified in calcined dolomite than in the modified pellets. In the large pore sizes, there were no significant differences between the three samples, however, a decrease of the mesopores was seen in the Zr doped sorbents comparing to calcine dolomite. Although larger mesopores were detected in the Zr modified sorbent, the bimodal distribution was maintained. The larger mesopores of calcined dolomite corresponds also with its higher surface area and hence, higher initial activity.

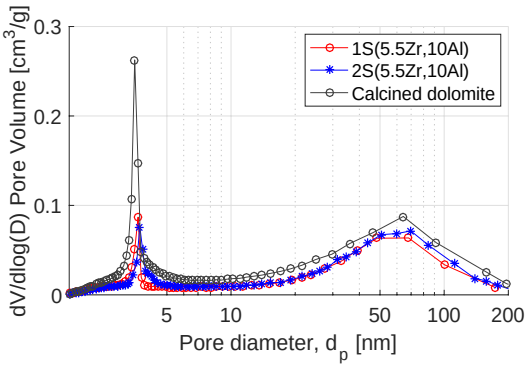

Figure 3: Pore diameter distribution of 1S(5.5Zr,10Al), 2S(5.5Zr,10Al) and calcined dolomite

It has been demonstrated that the smaller pores contribute more in the reaction-controlled regime, while the bigger pores in the diffusional regime [34]. This reveals the importance of maintaining small micropores throughout calcination-regeneration cycles in order to have an active and stable sorbent where fast kinetic and short times of carbonation are required (around 5 min) as in the CaL process. The evolution of pore volume distribution of 1S(5.5Zr, 10Al) during cycles (fresh, cycle 3 and 20) was analyzed in Figure 4. While the small sizes were closer to 3 nm in the fresh samples, they turned a bit bigger (around 5 nm) in the spent samples. Furthermore, the larger maximum pores shift from a peak at about 50 nm

to a peak around 100 nm. The changes in the sorbents surface area and pore-structure during cycles can indicate that a small degree of pore collapse occurs during carbonation-regeneration cycles. It is important to notice that the pores kept their bimodal distribution, with small mesopores. It was also identified a small decrease in the surface area from 8.8 m^2/g in the fresh sample to 8.4 and 7.6 m^2/g for the sample exposed to 3 a 20 cycle respectively, which indicates that even than a redistribution of the pores can arise, they are able to keep relatively good porous structure and surface area throughout the calcination-regeneration cycles. However, an interesting technique for the improvement can be the additions of pore generators during the synthesis as has been demonstrated [39,40].

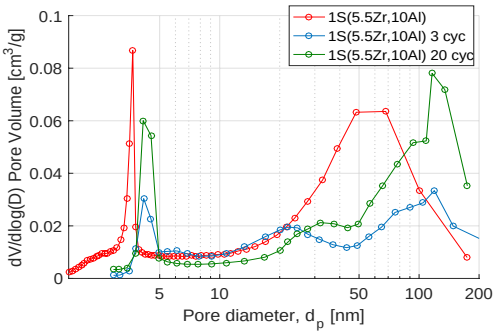

Figure 4: Pore volume distribution of 1Sa(5.5Zr,10Al), including fresh and spent sorbent after 3 and 20 carbonation-regeneration cycles

In order to gain further insight concerning the surface morphology, SEM-EDS analysis was done. Figures 5 and 6 show a selection of images from fresh and spent samples (after 40 carbonation/calcination cycles) for 1S(15Al), 1S(5.5Zr,10Al) and 2S(5.5Zr,10Al).

The images taken for fresh samples showed a great similarity with the ones found in the literature [29,39], especially for the image taken to 1S(15Al) where the calcium aluminate framework was clearly detected (Figure 5), forming stable cross-linked framework where possibly, the CaO grains are surrounded in the framework.

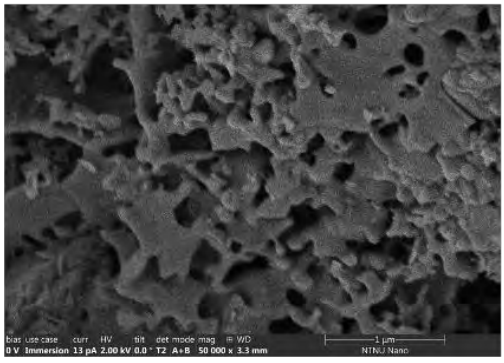

Figure 5: SEM images of 1S(15Al)

On the other hand, in the Zr-modified sorbents more compact structure was detected in 1S(5.5Zr,10Al) (Figure 6) comparing to 2S(5.5Zr,10Al) (Figure 7).This is on agreement with the slightly lower BET surface observed for 1S(5.5Zr,10Al) (Table 2). Hence, this can be a cause of the lower capture capacity obtained for 1S(5.5Zr,10Al) than for 2S(5.5Zr,10Al) as was pointed by Wei et al. [34]. Conversely, the sorbents prepared by 2S route presented and intermediate structure, where the calcium aluminate framework was detected forming a more opened structure. Simultaneously, the $CaZrO_3$ particle effect also was clearly seen forming a rougher structure which can be the responsible of the prevention of sintering [24].

In agreement with the XRD and the N_2 adsorption-desorption measurements, the images demonstrated that not major differences between the fresh and spent sorbents were observed, especially in the sorbents modified with Zr and prepared by 2-step route (2S(5.5,10Al) where the surface morphology seems appropriate to reach an acceptable capture capacity and maintained it through several carbonation-regeneration cycles.

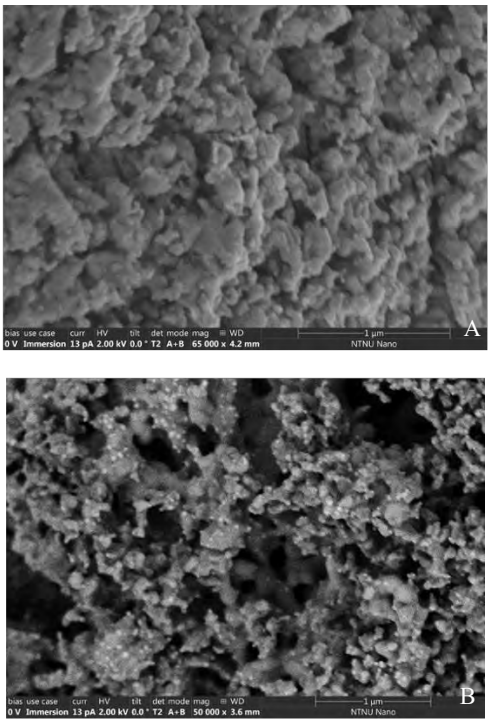

Figure 6: SEM images of 1S(5.5Zr,10Al) (fresh (A) and spent after 40 carbonation-calcination(B))

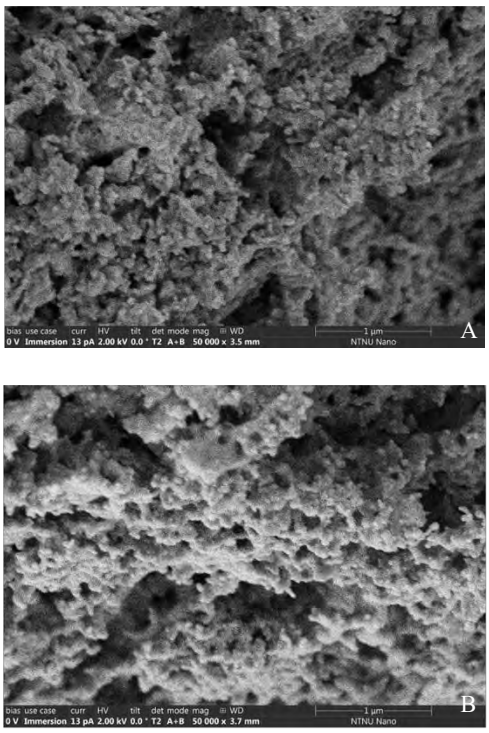

Figure 7: SEM images of 2S(5.5Zr,10Al) (fresh (A) and spent sorbent after 40 carbonation-calcination (B))

Finally, the distribution of the compounds was analyzed by the EDS mapping (Figure 8 and 9). It is known the importance of having a well dispersed $CaZrO_3$ particles in order to reach a good activity and stability [41]. In the images, the elemental mapping of Ca, Al, Zr Mg and O are represented. As expected, Ca is well dispersed in both sorbents. On the other hand, Mg and Al zones can be distinguished, which belongs to the areas rich on dolomite and cement respectively. These areas are clearly more divided in the sorbent synthetized by 1-step than 2-step route, indicating a worse homogeneous distribution of materials. Furthermore, the Zr is clearly not well dispersed also in this sorbent 1S(5.5Zr,10Al). This could explain the worse capture capacity shown by 1S(5.5Zr,10Al) comparing to 2S(5.5Zr,10Al). The sorbent synthetized by 2-step clearly present a better homogeneity and Zr dispersion. Hence, the higher capacity and slightly better stability of 2S(5.5Zr,10Al) can be attributed to the slightly higher surface area obtained, probably due to the better homogeneity as well as to the better Zr dispersion.

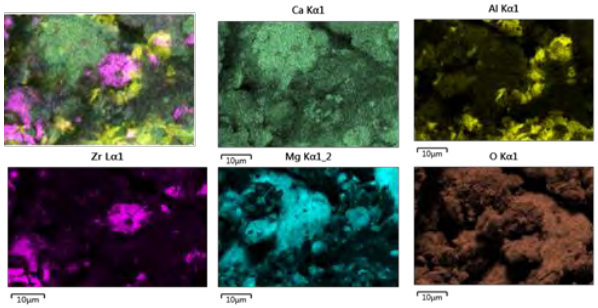

Figure 8: Elemental mapping of 1S(5.5Zr,10Al)

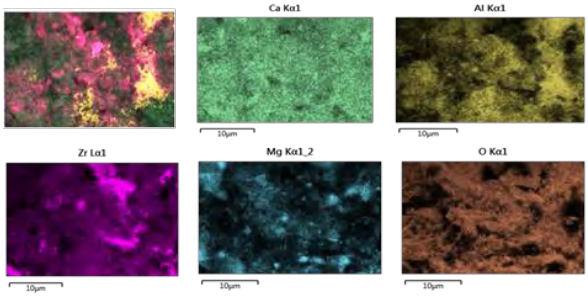

Figure 9: Elemental mapping of 2S(5.5Zr,10Al)

4. Conclusions

The results obtained in this work are shown as really promising. It has been observed that Zr is an interesting modifier comparing with Ce. The relatively high stability observed, for Zr modified sorbents, especially for 2S(5.5Zr,10Al) sorbent, is attributed mainly to two aspects. Firstly, to the formation of a mayenite framework which stabilize and, at the same time acts as a good binder. And secondly, to the formation of a relatively well dispersed $CaZrO_3$, which creates a barrier between CaO particles preventing the sintering and pore blockage. Regarding the two different synthesis routes employed (1-step and 2-step), the sorbent prepared by 2S route appears as the most active, mainly because of a more optimal dispersion of the Zr in the sorbent.

On the other hand, pellets were synthesized through manual pelletization in this work, but likewise, the method could be used to make mechanically strong sorbent by means of granulation-pelletization method, something that is already being investigated with promising results as well. Further exploration must be done including more realistic conditions to mimic the real process, including short carbonation times, higher carbonation/regeneration ramps and long-term experiments. Lastly, the simplicity of the synthesis procedure permits an easy scaling up.

5. References

[1] United Nations, United Nations Framew. Conv. Clim. Chang. (2015) 27–52.

[2] I.E. Agency, (2017).

[3] F. Winter, R.A. Agarwal, J. Hrdlicka, S. Varjani, (2019) 1–3.

[4] N.E. Flø, L. Faramarzi, T. De Cazenove, O.A. Hvidsten, A.K. Morken, E.S. Hamborg, K. Vernstad, G. Watson, S. Pedersen, T. Cents, B.F. Fostås, M.I. Shah, G. Lombardo, E. Gjernes, Energy Procedia 114 (2017) 1307–1324.

[5] J. Kittel, R. Idem, D. Gelowitz, P. Tontiwachwuthikul, G. Parrain, A. Bonneau, Energy Procedia 1 (2009) 791–797.

[6] P. Folger, Geol. Carbon Dioxide Storage (2012) 17–52.

[7] K. Atsonios, P. Grammelis, S.K. Antiohos, N. Nikolopoulos, E. Kakaras, Fuel 153 (2015) 210–223.

[8] D.P. Hanak, C. Biliyok, V. Manovic, Energy Environ. Sci. 9 (2016) 971–983.

[9] D. Berstad, R. Anantharaman, K. Jordal, Int. J. Greenh. Gas Control 11 (2012) 25–33.

[10] C.C. Cormos, Appl. Therm. Eng. 82 (2015) 120–128.

[11] A. Perejón, L.M. Romeo, Y. Lara, P. Lisbona, A. Martínez, J.M. Valverde, Appl. Energy 162 (2016) 787–807.

[12] D. Berstad, R. Anantharaman, R. Blom, K. Jordal, B. Arstad, Int. J. Greenh. Gas Control 24 (2014) 43–53.

[13] A.S.R. Subramanian, K. Jordal, R. Anantharaman, B.A.L. Hagen, S. Roussanaly, Energy Procedia 114 (2017) 2631–2641.

[14] J.M.G. Amann, C. Bouallou, Energy Procedia 1 (2009) 909–916.

[15] F. Donat, N.H. Florin, E.J. Anthony, P.S. Fennell, Environ. Sci. Technol. 46 (2012) 1262–1269.

[16] C. Luo, Y. Zheng, N. Ding, Q. Wu, G. Bian, C. Zheng, Ind. Eng. Chem. Res. 49 (2010) 11778–11784.

[17] J. Chen, L. Duan, Z. Sun, Energy & Fuels (2020).

[18] J.M. Valverde, P.E. Sanchez-Jimenez, L.A. Perez-Maqueda, Appl. Energy 138 (2015) 202–215.

[19] J.M. Valverde, J. Mater. Chem. A 1 (2013) 447–468.

[20] H.J. Yoon, K.B. Lee, Chem. Eng. J. 355 (2019) 850–857.

[21] H. R. Radfarnia, M. C. Iliuta, Ind. & Eng. Chem. Res. 51 (2012) 10390–10398.

[22] A. Antzara, E. Heracleous, A.A. Lemonidou, Energy Procedia 63 (2014) 2160–2169.

[23] R. Koirala, G.K. Reddy, J.Y. Lee, P.G. Smirniotis, Sep. Sci. Technol. 49 (2014) 47–54.

[24] X. He, G. Ji, T. Liu, M. Zhao, Energy and Fuels 33 (2019) 9996–10003.

[25] I. Yanase, T. Maeda, H. Kobayashi, Chem. Eng. J. 327 (2017) 548–554.

[26] V. Manovic, E.J. Anthony, Energy and Fuels 23 (2009) 4797–4804.

[27] V. Manovic, E. J. Anthony, Environ. Sci. & Technol. 43 (2009) 7117–7122.

[28] M. Erans, T. Beisheim, V. Manovic, M. Jeremias, K. Patchigolla, H. Dieter, L. Duan, E.J. Anthony, Faraday Discuss. 192 (2016) 97–111.

[29] L. Duan, Z. Yu, M. Erans, Y. Li, V. Manovic, E. J. Anthony, Ind. & Eng. Chem. Res. 55 (2016) 9476–9484.

[30] V. Manovic, E. J. Anthony, Ind. & Eng. Chem. Res. 48 (2009) 8906–8912.

[31] Y. Xu, C. Luo, Y. Zheng, H. Ding, L. Zhang, Energy & Fuels 30 (2016) 3219–3226.

[32] R. Koirala, K.R. Gunugunuri, S.E. Pratsinis, P.G. Smirniotis, J. Phys. Chem. C 115 (2011) 24804–24812.

[33] R. Zsigmondy, P. Scherrer, Kolloidchem. Ein Lehrb. 277 (1912) 387–409.

[34] S. Wei, R. Han, Y. Su, J. Gao, G. Zhao, Y. Qin, Energy and Fuels 33 (2019) 5398–5407.

[35] M. Erans, V. Manovic, E.J. Anthony, Appl. Energy 180 (2016) 722–742.

[36] A.H. Soleimanisalim, M.H. Sedghkerdar, D. Karami, N. Mahinpey, A.N. Antzara, A. Arregi, E. Heracleous, A.A. Lemonidou, Chem. Eng. J. 333 (2018) 5395–5402.

[37] C. Chen, S.T. Yang, W.S. Ahn, Mater. Lett. 75 (2012) 140–142.

[38] H. Chen, C. Zhao, Y. Yang, Fuel Process. Technol. 116 (2013) 116–122.

[39] L. Duan, C. Su, M. Erans, Y. Li, E.J. Anthony, H. Chen, Ind. Eng. Chem. Res. 55 (2016) 10294–10300.

[40] X. Tong, W. Liu, Y. Yang, J. Sun, Y. Hu, H. Chen, Q. Li, Fuel Process. Technol. 193 (2019) 149–158.

[41] H. Guo, S. Wang, C. Li, Y. Zhao, Q. Sun, X. Ma, Ind. Eng. Chem. Res. 55 (2016) 7873–7879.